Quantum Physics Letters
An International Journal

http://dx.doi.org/10.18576/qpl/060301

Microscopic Analysis of Elastic Scattering of ^{7}Be + ^{9}Be, ^{10}B, ^{12}C, ^{14}N, ^{27}Al, ^{58}Ni and ^{208}Pb Systems

M. Aygun[1,*], *O. Bayrak*[2], *and Z. Aygun* [3]

[1] Department of Physics, Bitlis Eren University, Bitlis, Turkey
[2] Department of Physics, Akdeniz University, Antalya, Turkey
[3] Vocational School of Technical Sciences, Bitlis Eren University, Bitlis, Turkey

Received: 12 Oct. 2017, Revised: 12 Nov. 2017, Accepted: 23 Nov. 2017
Published online: 1 Dec. 2017

Abstract: We investigate the elastic scattering angular distributions of ^{7}Be nucleus by ^{9}Be, ^{10}B, ^{12}C, ^{14}N, ^{27}Al, ^{58}Ni and ^{208}Pb target nuclei. The analysis is performed by using the double folding (DF) model with density-dependent and density-independent effective nucleon-nucleon (NN) interactions based on the M3Y interaction. The results are compared with each other as well as the experimental data. Then, simple formulas for the imaginary potential depth are proposed, for the first time, to use in the folding model calculations of the ^{7}Be-nucleus interactions.

Keywords: Optical model, Double folding model, Elastic scattering

1 Introduction

^{7}Be is known as a weakly bound nucleus with a separation energy of 1.59 MeV [1]. ^{7}Be, a half-life of 53.2 d, is a radioactive nucleus and is considered as core of ^{8}B nucleus. ^{7}Be has an important place in examining the interactions of weakly bound projectiles in research fields of nuclear physics. Various experimental and theoretical studies have been carried out on the interactions of ^{7}Be projectile with different target nuclei. For example, the scattering data of ^{7}Be + ^{9}Be reaction were measured at E_{lab}=17, 19 and 21 MeV in the angular range $24^{\circ} \leq \theta_{c.m.} \leq 57^{\circ}$ [2,3]. Elastic scattering data of ^{7}Be + ^{10}B (at 84 MeV) and ^{7}Be + ^{14}N (at 85 MeV) reactions were recorded by Azhari et al. [4]. Elastic scattering data of ^{7}Be by ^{12}C at incident energies of 18.8, 140 and 280 MeV were reported and investigated by using Woods-Saxon (WS) and the double folding (DF) potentials based on the optical model (OM) [5,6,7]. Kalita et al. [8] measured quasi-elastic scattering data of ^{7}Be + ^{27}Al reaction in the angular range $12^{\circ} \leq \theta_{c.m.} \leq 43^{\circ}$ in steps of 5° at 17, 19, and 21 MeV in order to compare ^{7}Be + ^{27}Al and ^{7}Li + ^{27}Al systems. Aguilera et al. [9] reported elastic scattering data of ^{7}Be on ^{58}Ni at different energies. The theoretical analysis for these data were conducted within the framework of the OM. ^{7}Be elastic scattering by ^{208}Pb at $E_{c.m.}$=121 MeV was measured [10] and analyzed by using global ^{7}Li parameters of Cook [11] as a starting point. However, ^{7}Be needs more experimental data for different target nuclei.

As far as we know, a comprehensive theoretical analysis of the elastic scattering of ^{7}Be with different target nuclei over the existing studies in the literature has not been evaluated for the same potential geometry. As a result of this, there is no global optical potential parameters for ^{7}Be nucleus. The analysis of experimental data has been started with literature values such as ^{7}Li nucleus in first stage. Then, a agreement fit with the experimental data has been obtained by searching the potential parameters. To address this deficiency, we focus on theoretical analysis of elastic scattering of ^{7}Be-nucleus reactions based on the OM. Such a work will be important and valuable in the calculations of elastic scattering, inelastic scattering, transfer reactions, coupled channels, etc. of ^{7}Be nucleus.

In the present work, we investigate angular distributions of elastic scattering of ^{7}Be projectile scattered from ^{9}Be, ^{10}B, ^{12}C, ^{14}N, ^{27}Al, ^{58}Ni and ^{208}Pb different target nuclei in a comprehensive manner. For this, we use four different nuclear potentials within the framework of the OM. Firstly, we assume the DF

* Corresponding author e-mail: murata.25@gmail.com

potential with M3Y interaction for the real part and WS potential with three free parameters for imaginary part. Secondly, we use the DF potential with M3Y interaction for both real and imaginary parts. Thirdly, we evaluate the DF potential with DDM3Y interaction for real part and WS potential for imaginary part. Finally, we apply the DF potential with DDM3Y interaction for both real and imaginary parts. From these calculations, we acquire a unique set of potential parameters describing the data. We compare our results with the experimental data.

In section 2, we give a brief description of theoretical formalism. In section 3, we mention the results of the calculations. In section 4, we present the summary and conclusions.

2 Theoretical Formalism

In first approach, real and imaginary parts of optical potential have been taken as the density-independent M3Y effective interaction, which well reproduces a lot of reaction data [12,13,14,15,16,17]. In this manner, the real potential is written

$$V_{\rm DF}^{M3Y}(\mathbf{r}) = \int d\mathbf{r}_1 \int d\mathbf{r}_2 \rho_P(\mathbf{r}_1)\rho_T(\mathbf{r}_2)v_{NN}(\mathbf{r}_{12}), \quad (1)$$

where $\mathbf{r}_{12} = \mathbf{r} - \mathbf{r}_1 + \mathbf{r}_2$, $v_{NN}(\mathbf{r}_{12})$ is the effective NN interaction, $\rho_P(\mathbf{r}_1)$ and $\rho_T(\mathbf{r}_2)$ are the density distributions of projectile and target nucleus, respectively. Density distribution of ^{7}Be projectile has been taken the Variational Monte Carlo (VMC) density distribution, which Pieper et al. [18] have reported ^{7}Be density obtained from the VMC calculations using the Argonne v18 (AV18) two-nucleon and Urbana X three-nucleon potentials (AV18+UX). This density has been displayed on both a logarithmic scale (small panel) and a linear scale (big panel) in Fig. 1.

^{9}Be density distribution has been assumed as [19]

$$\rho(r) = (\varsigma + \omega\eta^2 r^2)\exp(-\eta^2 r^2) + (\zeta + \varpi\chi^2 r^2)\exp(-\chi^2 r^2), \quad (2)$$

where $\varsigma = 0.0651$, $\omega = 0.0398$, $\eta = 0.5580$, $\zeta = 0.0544$, $\varpi = 0.0332$, and $\chi = 0.4878$.

The density distributions for ^{10}B, ^{12}C and ^{14}N target nuclei have been generated by

$$\rho(r) = (\xi + \gamma r^2)\exp(-\beta r^2). \quad (3)$$

ξ, γ and β values have been listed in Table 1.

To provide the density distributions of ^{27}Al, ^{58}Ni, and ^{208}Pb target nuclei, two-parameter Fermi (2pF) density has been used. It is given by

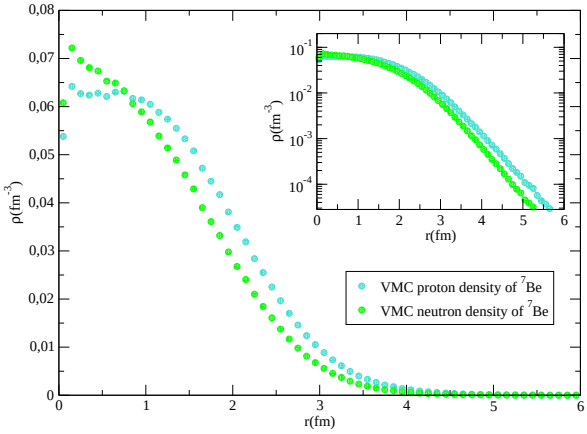

Fig. 1: The proton and neutron density distributions of ^{7}Be projectile in logarithmic scale (small panel) and linear scale (big panel)

$$\rho(r) = \frac{\rho_0}{1+\exp(\frac{r-c}{z})}. \quad (4)$$

ρ_0, c and z parameters for each nucleus have been presented in Table 1.

While v_{NN} is obtained, we have applied the M3Y nucleon-nucleon (Michigan 3 Yukawa) realistic interaction [20]

$$v_{NN}^{M3Y}(r) = 7999\,\frac{\exp(-4r)}{4r} - 2134\,\frac{\exp(-2.5r)}{2.5r} + J_{00}(E)\delta(r)\ \text{MeV}, \quad (5)$$

where $J_{00}(E)$ is the exchange term given by

$$J_{00}(E) = 276\,[1 - 0.005\,E_{\rm Lab}/A_p]\ \text{MeV fm}^3. \quad (6)$$

The imaginary potential has been taken as WS potential formulated by

$$W(r) = -W_0 f(r, R_w, a_w) \quad (7)$$

$$f(r, R_w, a_w) = \frac{1}{1+\exp(\frac{r-R_w}{a_w})}, \quad (8)$$

where $R_w = r_w\,(A_P^{1/3} + A_T^{1/3})$ and A_P (A_T) are mass numbers of projectile (target) nuclei. In the present study, this potential is called as DF(R).

In second approach, the imaginary potential of the optical potential is handled as folded potential multiplied by a normalization factor N_I while the real potential is thought as the DF potential. Thus, the real and imaginary potentials are in the same shape and different strengths. This potential is in the following form

$$U(R) = V_C(R) - (N_R + N_I)V_{\rm DF}. \quad (9)$$

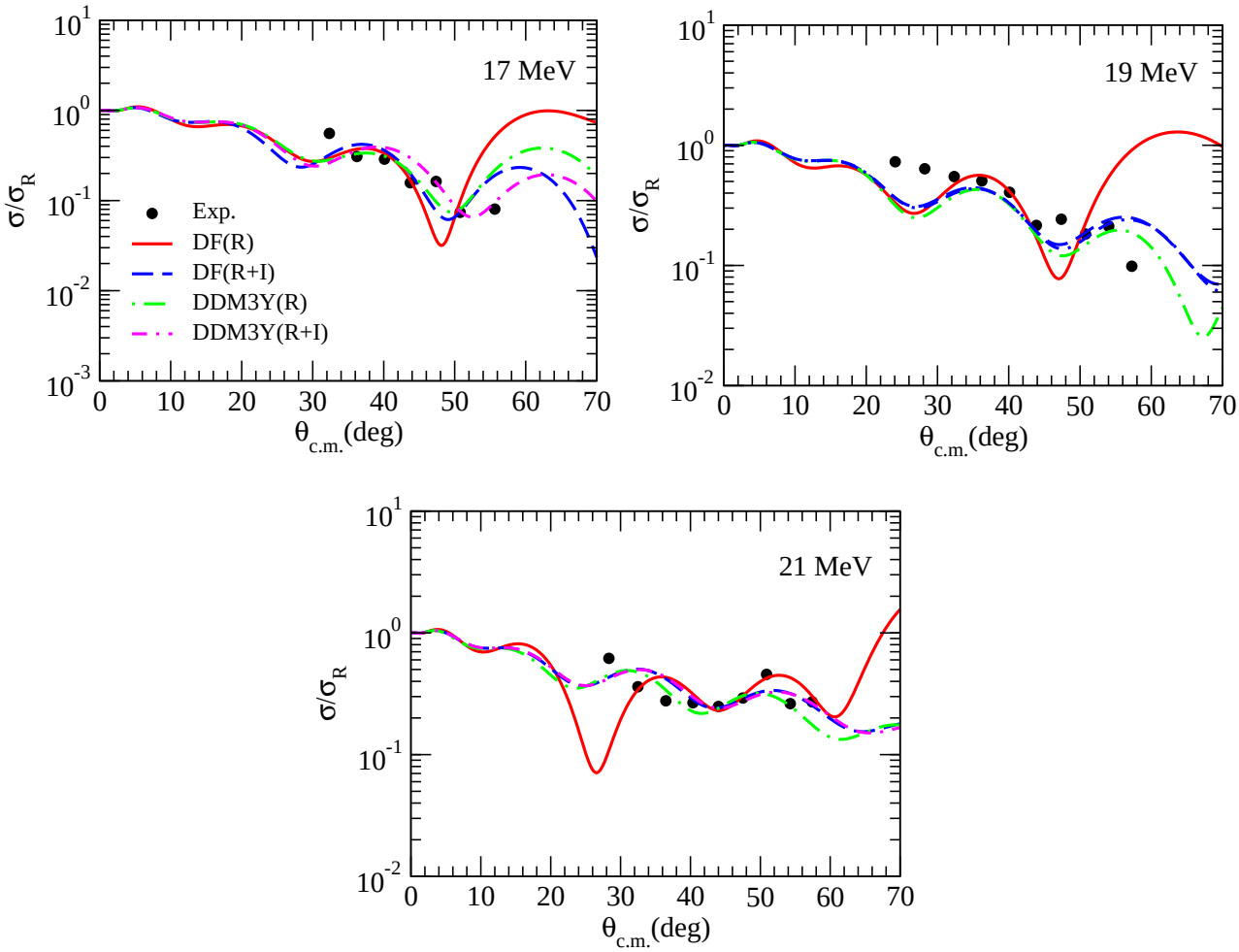

Fig. 2: The elastic scattering angular distributions of ^{7}Be + ^{9}Be reaction for DF(R), DF(R+I), DDM3Y(R) and DDM3Y(R+I) potentials in comparison with the experimental data at 17, 19 and 21 MeV. The experimental data are from Refs. [2,3].

Table 1: The parameters of 2pF density distribution for ^{27}Al, ^{58}Ni and ^{208}Pb nuclei, and the parameters of gaussian density distribution for ^{10}B, ^{12}C, ^{14}N nuclei.

		2pF					Gaussian		
Nucleus	c	z	ρ_0	Ref.	Nucleus	ξ	γ	β	Ref.
^{27}Al	2.84	0.569	0.2015	[23]	^{10}B	0.15924	0.045519	0.341991	[25]
^{58}Ni	4.094	0.54	0.172	[24]	^{12}C	0.17261	0.064712	0.351376	[25]
^{208}Pb	6.62	0.551	0.1600	[23]	^{14}N	0.1660	0.07171	0.3350	[26]

and, is represented as DF(R+I) in our work.

In third approach, the real part of optical potential has been evaluated as the density-dependent M3Y effective interaction which is known as DDM3Y interaction. For this, total potential is shown by

$$V_{\rm DF}^{DDM3Y}(\mathbf{r}) = \int d\mathbf{r}_1 \int d\mathbf{r}_2 \rho_P(\mathbf{r}_1)\rho_T(\mathbf{r}_2)v_{NN}(\mathbf{r}_{12}), \quad (10)$$

Here, the M3Y interaction has density dependence form given by

$$v_{NN}^{DDM3Y}(r,\rho,E) = f(\rho,E)v_{NN}(r) \quad (11)$$

where $v_{NN}(r)$ is the M3Y interaction described above and $f(\rho,E)$ is parameterized by

$$f(\rho,E) = C(E)[1+\alpha(E)e^{-\beta(E)\rho}] \quad (12)$$

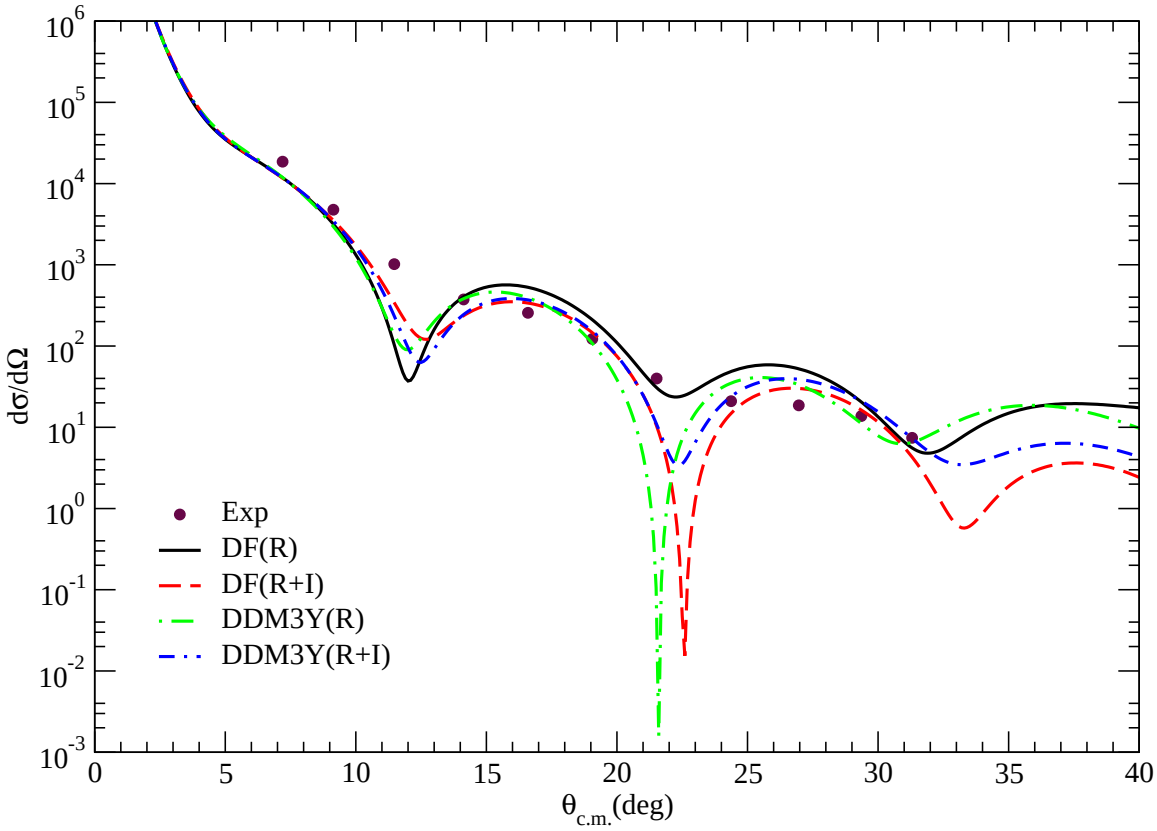

Fig. 3: The same as Fig. 2 but for ^{7}Be + ^{10}B reaction at 84 MeV. The experimental data are from Ref. [4].

Table 2: The optical potential parameters and real and imaginary volume integrals obtained from analysis with DF(R) potential of elastic scattering of ^{7}Be from ^{9}Be, ^{10}B, ^{12}C, ^{14}N, ^{27}Al, ^{58}Ni and ^{208}Pb.

System	Energy *MeV*	N_R	W_0 *MeV*	r_w *fm*	a_w *fm*	J_v *MeV.fm*^{3}	J_w *MeV.fm*^{3}
	17	0.750	1.55	1.3	0.6	346.4	16.3
^{7}Be + ^{9}Be	19	1.080	1.60	1.3	0.6	498.8	16.8
	21	0.925	1.93	1.3	0.6	427.2	20.3
^{7}Be + ^{10}B	84	1.0	7.0	1.3	0.6	415.7	69.8
	18.8	1.01	1.50	1.3	0.6	349.8	13.6
^{7}Be + ^{12}C	140	1.00	11.5	1.3	0.6	346.4	104.6
	280	0.80	11.7	1.3	0.6	277.1	106.5
^{7}Be + ^{14}N	85	1.0	17.0	1.3	0.6	296.9	143.5
	13.8	1.00	1.00	1.3	0.6	153.9	6.3
	15.2	0.98	1.10	1.3	0.6	150.9	6.9
^{7}Be + ^{27}Al	17	1.02	1.20	1.3	0.6	157.0	7.5
	19	1.01	1.50	1.3	0.6	155.5	9.4
	21	1.05	4.50	1.3	0.6	161.6	28.2
	17.1	1.11	16.1	1.3	0.6	79.5	75.0
^{7}Be + ^{58}Ni	18.5	0.88	16.5	1.3	0.6	63.1	76.9
	19.9	1.00	16.9	1.3	0.6	71.7	78.8
	21.4	0.89	20.0	1.3	0.6	63.8	93.2
^{7}Be + ^{208}Pb	125.07	1.19	24.0	1.3	0.6	23.8	75.5

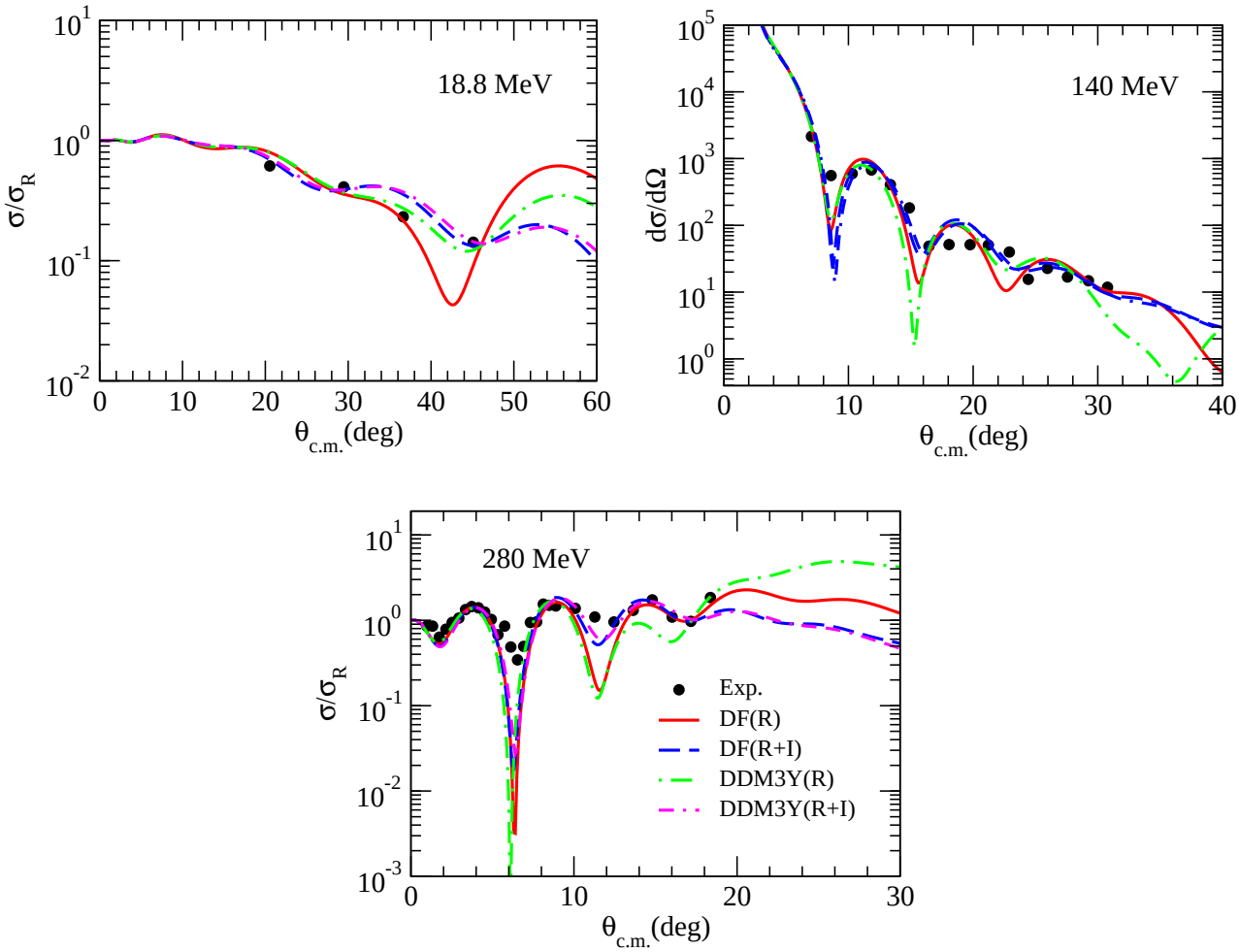

Fig. 4: The same as Fig. 2 but for ^{7}Be + ^{12}C reaction at 18.8, 140 and 280 MeV. The experimental data are from Refs. [5,6,7].

where $\rho(r_1,r_2)=\rho_1(r_1)+\rho_2(r_2)$. The parameters C, α and β are 0.2845, 3.6391 and 2.9605, respectively [21]. This potential is arisen as DDM3Y(R) in our work.

In fourth approach, the imaginary potential is assumed as folded potential multiplied by a normalization factor N_I, and the real potential is in the DF potential form. In this manner, both real and imaginary potentials have been considered in the same shape but different strengths, which are given by

$$U(R)=V_C(R)-(N_R+N_I)V_{\rm DF}^{DDM3Y}. \qquad (13)$$

This potential is denoted to DDM3Y(R+I) in our work. The program FRESCO [22] is used for the theoretical calculations.

3 Results and Discussion

We have investigated elastic scattering angular distributions of ^{7}Be projectile by ^{9}Be, ^{10}B, ^{12}C, ^{14}N, ^{27}Al, ^{58}Ni and ^{208}Pb target nuclei. For this purpose, we have used four different approaches. In first (DF(R)) and third (DDM3Y(R)) approaches, the optical potential parameters have been researched to obtain good agreement results with the experimental data. To study in the same potential geometry, r_w and a_w values have been fixed for all the investigated reactions. After the test calculations in steps of 0.1 and 0.01 fm, r_w and a_w values have been taken as 1.3 fm and 0.6 fm for the DF(R) approach and 1.4 fm and 0.7 fm for the DDM3Y(R) approach, respectively. Then, N_R and W_0 values have been searched. The optical potential parameters obtained for all the reactions in terms of DF(R) and DDM3Y(R) have been listed in Tables 2 and 4, respectively.

In second (DF(R+I)) and fourth (DDM3Y(R+I)) approaches, the real and imaginary parts of the optical potential have been multiplied with N_R and N_I normalization factors. These values have been investigated to obtain the behavior of the experimental

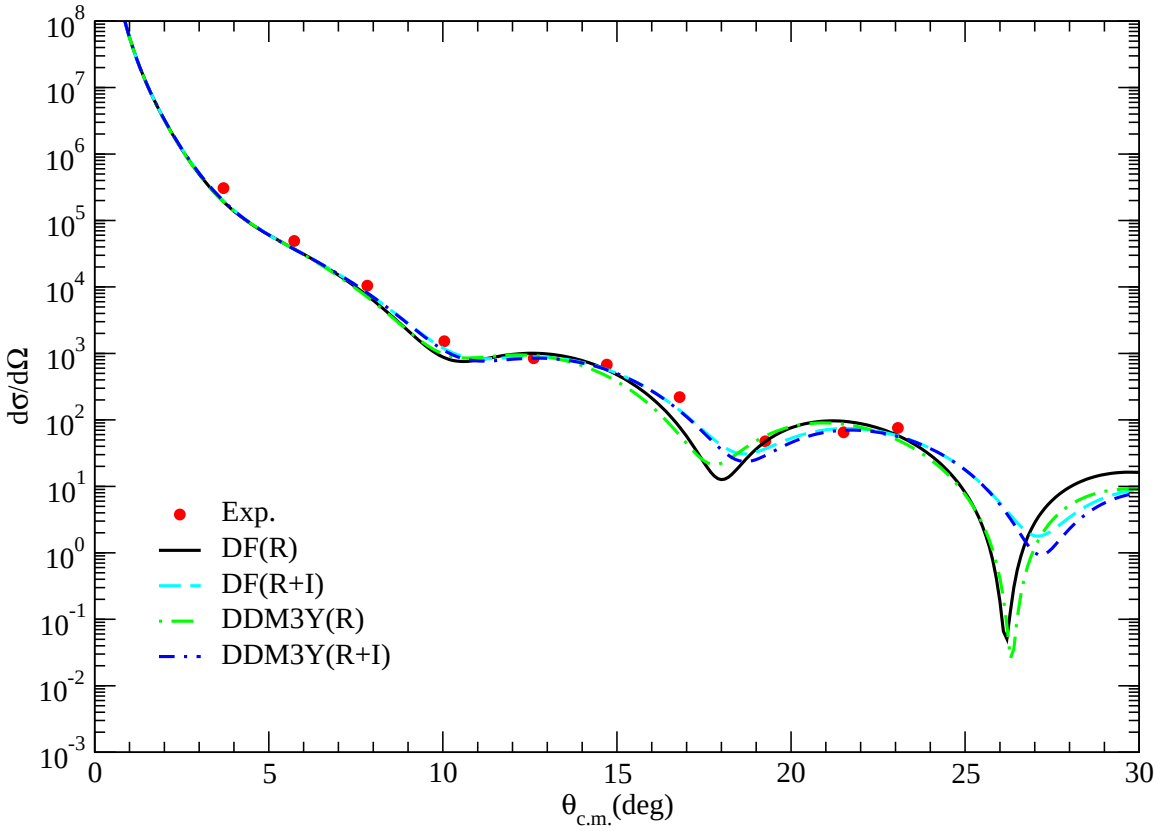

Fig. 5: The same as Fig. 2 but for ^{7}Be + ^{14}N reaction at 85 MeV. The experimental data are from Ref. [4].

Table 3: The normalization factors (N_R and N_I), real and imaginary volume integrals obtained from analysis with DF(R+I) potential of elastic scattering of ^{7}Be from ^{9}Be, ^{10}B, ^{12}C, ^{14}N, ^{27}Al, ^{58}Ni and ^{208}Pb.

System	Energy	N_R	N_I	J_v $MeV.fm^3$	J_w $MeV.fm^3$
	17	1.35	0.40	623.5	184.7
^{7}Be + ^{9}Be	19	0.85	0.90	392.6	415.7
	21	0.60	1.35	277.1	623.5
^{7}Be + ^{10}B	84	0.65	0.65	270.2	270.2
	18.8	1.40	0.45	484.9	155.9
^{7}Be + ^{12}C	140	1.00	0.50	346.4	173.2
	280	1.00	0.56	346.4	194.0
^{7}Be + ^{14}N	85	0.6	1.0	178.1	296.9
	13.8	1.30	1.30	200.1	200.1
	15.2	1.40	0.75	215.6	115.5
^{7}Be + ^{27}Al	17	1.30	1.30	200.1	200.1
	19	1.00	1.00	154.0	154.0
	21	1.25	0.35	192.4	53.9
	17.1	1.00	1.00	71.6	71.6
^{7}Be + ^{58}Ni	18.5	0.82	0.90	58.8	64.5
	19.9	0.82	1.10	58.8	78.9
	21.4	0.80	1.00	57.3	71.7
^{7}Be + ^{208}Pb	125.07	1.00	1.25	20.0	25.0

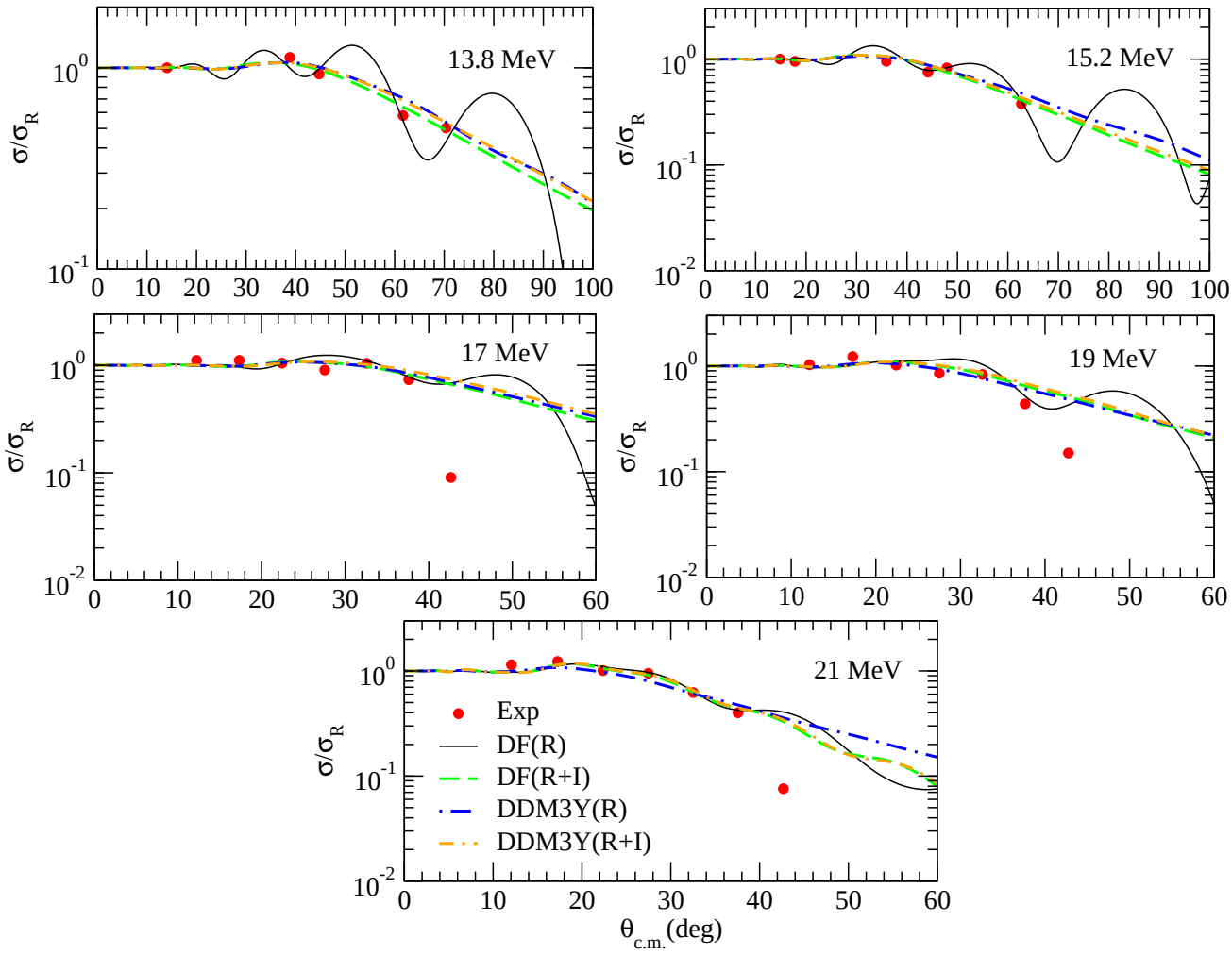

Fig. 6: The same as Fig. 2 but for ^{7}Be + ^{27}Al reaction at 13.8, 15.2, 17, 19 and 21 MeV. The experimental data are from Refs. [8,27].

data. N_R and N_I values for all the systems analyzed with this work have been given in Tables 3 and 5.

Angular distributions of ^{7}Be + ^{9}Be system have been investigated at incident energies of 17, 19 and 21 MeV. The theoretical results, obtained for four different nuclear potentials, have been plotted in Fig. 2. In spite of oscillatory experimental data, our results are in agreement with the data in general.

The elastic scattering data of ^{7}Be on ^{10}B has been examined at 10 MeV. The analysis results of the system have been plotted for potentials evaluated in Fig. 3. The behaviors of DF(R+I) and DDM3Y(R+I) potentials are the same up to 22° but after 22° the results are different. However, it has been seen that the potentials well defines the experimental data except for DF(R).

Another reaction analyzed with this work is ^{7}Be + ^{12}C system at incident energies of 18.8, 140 and 280 MeV. The results obtained for DF(R), DF(R+I), DDM3Y(R) and DDM3Y(R+I) potentials by using the DF model have been shown in Fig. 4. Agreement between theoretical results and the experimental data is quite reasonable despite the oscillating structure of the experimental data.

The elastic scattering results of ^{7}Be + ^{14}N have been calculated via four kind potentials at 85 MeV and have appeared in comparative form in Fig. 5. It has been observed that the results are in good agreement with the experimental data. Especially, this harmony is excellent for DF(R+I) and DDM3Y(R+I) potentials.

The theoretical calculations of ^{7}Be elastic scattering by ^{27}Al as an example of light-heavy target nucleus have been carried out for DF(R), DF(R+I), DDM3Y(R) and DDM3Y(R+I) potentials within the framework of the DF model at incident energies of 13.8, 15.2, 17, 19 and 21 MeV. The theoretical results have been plotted comparatively with each other as well as the data in Fig.

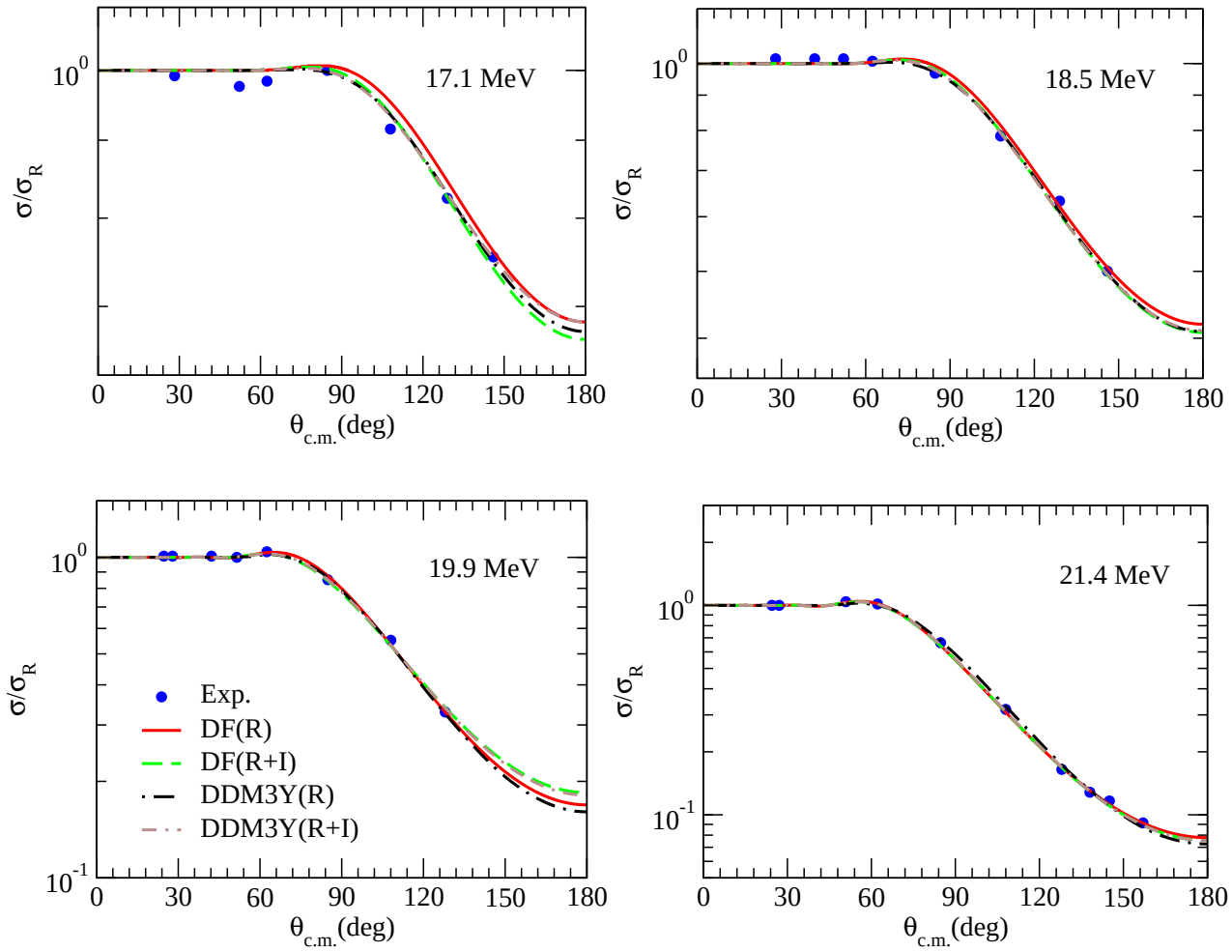

Fig. 7: The same as Fig. 2 but for ^{7}Be + ^{58}Ni reaction at 17.1, 18.5, 19.9 and 21.4 MeV. The experimental data are from Ref. [9].

6. It has been seen that agreement between theoretical results and the experimental data is quite reasonable.

^{7}Be + ^{58}Ni reaction has been investigated as an interaction with the medium mass target. The elastic scattering angular distributions have been obtained for different nuclear potentials at 17.1, 18.5, 19.9 and 21.4 MeV. The results have been exhibited with the experimental data in Fig. 7. It has been realized that agreement between our results and the data are almost perfect except for DF(R) results at 17.1 MeV.

Finally, elastic scattering interaction of ^{7}Be with ^{208}Pb nucleus as heavy target has been studied for DF(R), DF(R+I), DDM3Y(R) and DDM3Y(R+I) nuclear potentials by using the DF model at $E_{c.m.}$=121 MeV. The theoretical results have been shown in Fig. 8. It has been observed that the results are in agreement with the experimental data but not at forward angles.

In Tables 2-5, we have listed the real (J_v) and imaginary (J_w) volume integrals which are calculated by using the optical potential parameters obtained from the theoretical analysis. Then, we have given in a comparative manner the cross-sections (σ) of DF(R), DF(R+I), DDM3Y(R) and DDM3Y(R+I) potentials together with literature for all the reactions in Table 6. We have observed that the cross-sections of the potentials have shown a similar behavior with each other. That is, the cross-sections have displayed an increasing behavior with the incident energy for the systems except for ^{7}Be + ^{12}C reaction at 280 MeV. In addition to this, we have compared our cross-sections with the literature [3,27,8,9, 10] shown with Table 6. We have realized that the results of this work are very close to the literature values. Therefore, it can be said that the similar cross-sections acquired with different potentials are attributed to the harmony of the theoretical results.

In our work, for the first time, we propose new global imaginary potential equations to determine the depth of imaginary potential in DF(R) and DDM3Y(R) calculations based on the DFM while the elastic scattering interactions of ^{7}Be projectile with different

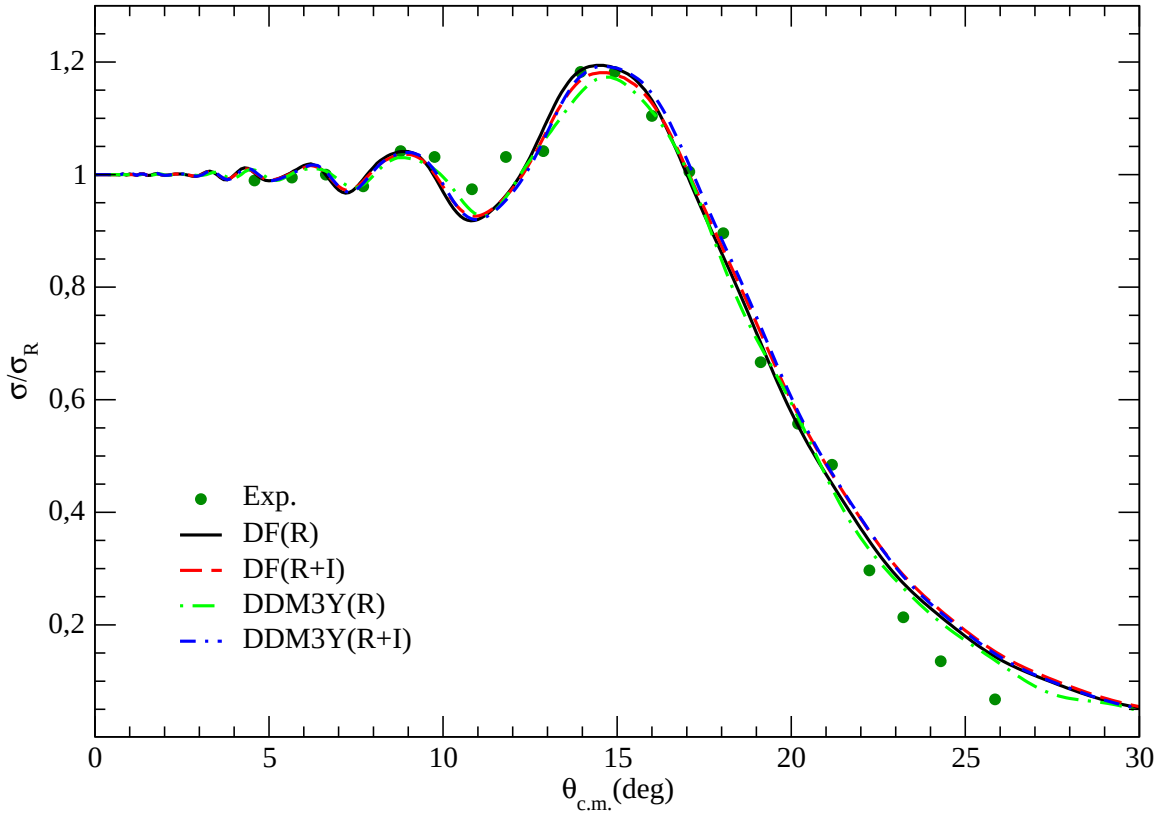

Fig. 8: The same as Fig. 2 but for ^{7}Be + ^{208}Pb reaction at 125.07 MeV. The experimental data are from Ref. [10].

Table 4: The same as Table 2 but for analysis with DDM3Y(R) potential.

System	Energy *MeV*	N_R	W_0 *MeV*	r_w *fm*	a_w *fm*	J_v *MeV.fm*^{3}	J_w *MeV.fm*^{3}
	17	0.85	4.20	1.4	0.7	392.6	56.3
^{7}Be + ^{9}Be	19	1.00	7.10	1.4	0.7	461.8	95.2
	21	1.00	18.5	1.4	0.7	461.8	248.1
^{7}Be + ^{10}B	84	1.0	7.00	1.4	0.7	415.7	88.9
	18.8	0.90	2.50	1.4	0.7	311.7	28.9
^{7}Be + ^{12}C	140	1.02	7.70	1.4	0.7	353.3	89.1
	280	1.00	8.70	1.4	0.7	346.4	100.7
^{7}Be + ^{14}N	85	1.00	10.0	1.4	0.7	296.9	107.3
	13.8	1.00	6.20	1.4	0.7	153.9	49.3
	15.2	1.00	7.00	1.4	0.7	153.9	55.6
^{7}Be + ^{27}Al	17	1.00	8.90	1.4	0.7	153.9	70.7
	19	1.00	15.5	1.4	0.7	153.9	123.2
	21	1.00	15.6	1.4	0.7	153.9	124.0
	17.1	1.00	5.30	1.4	0.7	71.7	31.2
^{7}Be + ^{58}Ni	18.5	0.78	5.40	1.4	0.7	55.9	31.8
	19.9	0.91	5.50	1.4	0.7	65.2	32.3
	21.4	0.65	5.60	1.4	0.7	46.6	32.9
^{7}Be + ^{208}Pb	125.07	1.05	7.50	1.4	0.7	21.0	29.7

target nuclei are examined. These equations change with the incident energy of ^{7}Be, charge number (Z_T) and mass number (A_T) of target nucleus. We have used the potential parameters listed in Tables 2 and 4 while these equations

Table 5: The same as Table 3 but for analysis with DDM3Y(R+I) potential.

System	Energy	N_R	N_I	J_v $MeV.fm^3$	J_w $MeV.fm^3$
^{7}Be + ^{9}Be	17	0.88	0.40	406.5	184.8
	19	0.90	0.90	415.6	415.6
	21	0.57	1.35	263.2	623.4
^{7}Be + ^{10}B	84	0.90	0.60	374.1	249.4
^{7}Be + ^{12}C	18.8	1.30	0.55	450.2	190.5
	140	1.00	0.50	346.4	173.2
	280	1.00	0.54	346.4	187.1
^{7}Be + ^{14}N	85	0.75	1.10	222.7	326.6
^{7}Be + ^{27}Al	13.8	1.20	1.20	184.7	184.7
	15.2	1.50	0.90	230.9	138.5
	17	1.00	1.00	153.9	153.9
	19	1.00	1.00	153.9	153.9
	21	1.40	0.35	215.5	53.9
^{7}Be + ^{58}Ni	17.1	1.00	1.40	71.7	100.4
	18.5	1.00	1.19	71.7	85.3
	19.9	1.06	1.30	75.9	93.1
	21.4	1.00	1.21	71.7	86.7
^{7}Be + ^{208}Pb	125.07	1.30	1.40	26.0	28.0

Table 6: The cross-sections (σ) obtained with DF(R), DF(R+I), DDM3Y(R), DDM3Y(R+I) nuclear potentials in comparison with the literature.

System	E_{Lab} MeV	$\sigma_{\mathrm{DF(R)}}$ mb	$\sigma_{\mathrm{DF(R+I)}}$ mb	$\sigma_{\mathrm{DDM3Y(R)}}$ mb	$\sigma_{\mathrm{DDM3Y(R+I)}}$ mb	$\sigma_{\mathrm{Literature}}$ mb
^{7}Be + ^{9}Be	17	905.7	1333.3	1221.1	1201.8	1298 - Ref.[3]
	19	803.1	1344.5	1362.3	1326.0	1445 - Ref.[3]
	21	970.3	1402.2	1570.5	1372.6	1562 - Ref.[3]
^{7}Be + ^{10}B	84	1144.0	1211.2	1335.2	1192.2	
^{7}Be + ^{12}C	18.8	784.0	1148.3	1012.2	1110.7	
	140	1257.1	1171.9	1352.2	1127.8	
	280	1138.6	1091.3	1255.9	1038.9	
^{7}Be + ^{14}N	85	1454.4	1396.5	1573.1	1387.7	
^{7}Be + ^{27}Al	13.8	347.2	751.9	668.4	671.5	741 ± 48 - Ref.[27]
	15.2	457.7	861.0	836.9	826.4	896 ± 71 - Ref.[27]
	17	606.6	1067.8	1035.0	930.5	772 - Ref.[8]
	19	686.7	1130.4	1294.9	1062.9	1010 - Ref.[8]
	21	1042.9	1149.5	1411.6	1105.4	1105 - Ref.[8]
^{7}Be + ^{58}Ni	17.1	69.9	85.1	89.6	87.5	106 ± 30 - Ref.[9]
	18.5	169.6	185.7	196.8	189.6	182 ± 26 - Ref.[9]
	19.9	331.6	359.9	359.7	355.1	330 ± 101 - Ref.[9]
	21.4	502.0	512.4	502.6	507.1	506 ± 97 - Ref.[9]
^{7}Be + ^{208}Pb	125.07	3050.7	3048.3	3160.0	3011.4	3182 - Ref.[10]

are obtained. Thus, our equations for DF(R) and DDM3Y(R) nuclear potentials are formulated by

$$W = -2.22698 + 0.0410954E + 1.89096\frac{Z_T}{A_T^{1/3}}, \quad \text{for DF(R) potential} \tag{14}$$

and

$$W = 9.43937 + 0.000728E - 0.26895\frac{Z_T}{A_T^{1/3}}, \quad \text{for DDM3Y(R) potential} \tag{15}$$

where E is the incident energy of ^{7}Be projectile.

4 Summary

In the present study, we have examined eighteen data sets of ^{7}Be nucleus scattered from seven different target nuclei at various incident energies at the same potential geometry. For this purpose, we have evaluated four different nuclear potentials such as DF(R), DF(R+I), DDM3Y(R) and DDM3Y(R+I) based on the DF model within the framework of the OM. We have achieved good agreement results with the experimental data. The theoretical results for some reactions are almost excellent. This indicates that a successful analysis of experimental data of ^{7}Be by different target nuclei has been performed in terms of DF(R), DF(R+I), DDM3Y(R) and DDM3Y(R+I) nuclear potentials. Thus, we can say that the OM parameters determined with our work will be useful in both theoretical and experimental studies of ^{7}Be-nucleus interactions.

In our research, also, we have derived new equations to find the imaginary potentials of DF(R) and DDM3Y(R) in examining the ^{7}Be-nucleus reactions. We think that these equations will be very valuable and applicable in the analysis of the nuclear interactions such as elastic scattering, inelastic scattering, coupled channels, transfer reactions etc.

References

[1] J. J. Kolata, V. Guimarães and E. F. Aguilera, Eur. Phys. J. A **52**, 123 (2016).
[2] S. Verma, J. J. Das, A. Jhingan, et al., Eur. Phys. J. ST **150**, 75-78 (2007).
[3] S. Verma, J. J. Das, A. Jhingan, et al., Eur. Phys. J. A **44**, 385-392 (2010).
[4] A. Azhari, V. Burjan, F. Carstoiu, et al., Phys. Rev. C **63**, 055803 (2001).
[5] T. Yamagata, K. Yuasa, N. Inabe, et al., Phys. Rev. C **39**, 873 (1989).
[6] A. Barioni, J. C. Zamora, V. Guimarães, et al., Phys. Rev. C **84**, 014603 (2011).
[7] I. Pecina, R. Anne, D. Bazin, et al., Phys. Rev. C **52**, 191 (1995).
[8] K. Kalita, S. Verma, R. Singh, et al., Phys. Rev. C **73**, 024609 (2006).
[9] E. F. Aguilera, E. Martinez-Quiroz, D. Lizcano, et al., Phys. Rev. C **79**, 021601(R) (2009).
[10] J. S. Wang, Y. Y. Yang, Q. Wang, et al., Journal of Physics: Conference Series **420**, 012075 (2013).
[11] J. Cook, Nucl. Phys. A **388**, 153 (1982).
[12] M. Aygun, I. Boztosun and Y. Sahin, Phys. At. Nucl. **75**, 963-968 (2012).
[13] M. Aygun, Ann. Nucl. Energy **51**, 1-4 (2013).
[14] M. Aygun, Eur. Phys. J. A **48**, 145 (2012).
[15] M. Aygun, I Boztosun and K Rusek, Mod. Phys. Lett. A **28**, 1350112 (2013).
[16] M. Aygun, Acta Phys. Pol. B **45**, 1875 (2014).
[17] M. Aygun, Chin. J. Phys. **53**, 080301 (2015).
[18] S. C. Pieper, K. Varga and R. B. Wiringa, Phys. Rev. C **66**, 044310 (2002).
[19] V. Hnizdo, J. Szymakowski, K. W. Kemper and J. D. Fox, Phys. Rev. C **24**, 1495 (1981).
[20] G. R. Satchler and W. G. Love, Phys. Rep. **55**, 183 (1979).
[21] D. T. Khoa and W. von Oertzen, Phys. Lett. B **342**, 6-12 (1995).
[22] I. J. Thompson, Computer Phys. Rep. **7**, 167 (1988).
[23] S. Hossain, M. N. A. Abdullah, Md. Zulfiker Rahman, A. K. Basak and F. B. Malik, Phys. Scr. **87**, 015201 (2013).
[24] M. El-Azab Farid and M. A. Hassanain, Nucl. Phys. A **678**, 39-75 (2000).
[25] C. W. Glover, K. W. Kemper, L. A. Parks, F. Petrovich and D. P. Stanley, Nucl. Phys. A **337**, 520-532 (1980).
[26] J. F. Mateja, D. P. Stanley, L. V. Theisen, A. D. Frawley, P. L. Pepmiller, L. R. Medsker and P. B. Nagel, Nucl. Phys. A **351**, 509-518 (1981).
[27] V. Morcelle, R. Lichtenthäler, R. Linares, et al., Phys. Rev. C **89**, 044611 (2014).